Atomization of a small-diameter liquid jet by a high-speed gas stream

Christopher M. Varga[1]
Juan C. Lasheras[1]
Emil J. Hopfinger[2]

[1]Department of Mechanical and Aerospace Engineering, University of California, San Diego, La Jolla, California, USA 92093-0411
[2]LEGI-CNRS/UJF/INPG, BP 53, 38041 Grenoble Cedex, France

The breakup and atomization of a small-diameter liquid jet by a high-speed coaxial gas stream has been investigated experimentally using high-speed video and phase-Doppler particle sizing techniques. Observations of the initial breakup of the liquid jet in the near-nozzle region, combined with measurements of both droplet size and velocity throughout the flow domain were utilized in an endeavor to elucidate the dominant mechanisms of both primary and secondary breakup in coaxial liquid-gas jet flows. High-speed images of the primary breakup process illustrate that when the aerodynamic Weber number and the gas-to-liquid momentum flux ratio are large, the bulk of the liquid atomization is completed within a few gas-jet diameters of the nozzle exit, inside of the potential cone of the gas flow. The liquid is reduced to a very fine mist through an aerodynamic stripping process which closely resembles that of a liquid drop suddenly exposed to a high-speed gas stream. These observations, along with an experimental analysis of the dependence of the mean droplet diameter on the gas velocity and surface tension, have implicated the Rayleigh-Taylor instability as the dominant mechanism of primary droplet formation. A phenomenological breakup model has been developed, which proposes that the primary droplet size should scale with the most amplified wavelength of the Rayleigh-Taylor instability. Predictions from this model have been shown to compare well with droplet-size measurements and instability wavelengths in the aerodynamic breakup of both water and ethanol jets. An analysis of the effect of relative acceleration of different droplet size classes has also been carried out as part of a broader study of secondary breakup mechanisms in the downstream evolution of mean droplet sizes in coaxial jets.

1. Introduction

The breakup and atomization of a liquid jet by a high-speed gas stream is multi-parameter, two-phase flow problem which continues to resist clear understanding. A recent review by Lasheras and Hopfinger [1] brings light to the many open questions which remain in this area of fluid mechanics. For combustion applications, empirical correlations for droplet sizes as a function of injection parameters are plentiful [2], however, detailed studies of the physical mechanisms responsible for these relationships are clearly needed in order to construct broadly applicable models.

The breakup and atomization of a liquid jet injected into a high-speed gas stream is fundamentally different from that which occurs for the same jet discharging into a stagnant gaseous environment. When the gas stream momentum flux is of the same order, or in excess of that of the liquid jet, the atomization is achieved through a kinetic energy transfer from the gas to the liquid. This type of atomization is known as air-assist atomization (when

air is the gas) [2], and a typical geometry for this type of atomization is one of a coaxial nature, shown schematically in Fig. 1. In this configuration, a round liquid jet of diameter D_l is atomized by an annular gas jet of outer diameter D_g, these streams having velocities of U_l and U_g, respectively. Practical applications of coaxial atomization are numerous, particular in combustion systems. In liquid-propellant rocket engines for example, a large number of coaxial atomizers are employed to supply the fuel and oxidizer for combustion [3].

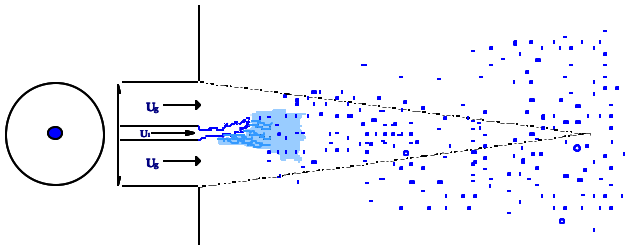

Figure 1 – Large-area ratio coaxial liquid-gas nozzle geometry

Empirical expressions in coaxial jet sprays are most often expressed in the form of power laws for the Sauter mean diameter (*SMD*) as a function of injection conditions; in particular, the dependence of mean droplet sizes as a function of the atomizing gas velocity are commonly expressed as $SMD \propto U_g^{-n}$, with n ranging from $0.7 = n = 1.5$. Physical arguments for particular values of the exponent n are generally lacking however.

The instability which occurs at the interface of parallel flowing gas and liquid streams has been studied by many investigators (e.g. [4][5][6][7][8]). Raynal [8] has shown that the wavelength of the instability which develops at the gas-liquid interface in coaxial jets ultimately depends on the gas vorticity thickness and the density ratio as $l_1 \mu d_g(r_l/r_g)^{1/2}$. Amplification of this primary wave structure leads to the formation of axisymmetric or helical wave sheets which eventually breakup into droplets. The mechanisms of formation and breakup of these wave sheets or liquid tongues are still poorly understood. These mechanisms are expected to depend strongly on the aerodynamic Weber number ($We = r_g (U_g - U_l)^2 D_l / s$), as is known from studies of drop breakup in high-speed gas streams [9][10][11].

Beyond the initial breakup region, secondary drop breakup mechanisms are generally necessary to explain the experimentally observed downstream variation of mean droplet sizes. Relative acceleration effects have mostly been ignored in spray studies to date; the unavoidable creation of a polydisperse droplet-size distribution in the primary breakup process gives rise to a situation wherein different droplet size classes respond differently to the surrounding high-speed gas. Differences in the acceleration of different size droplets can lead to non-trivial downstream variations in the mean droplet diameter through a 'convective shuffling' effect.

2. Experimental setup

The flow configuration chosen for this study was shown in Fig. 1, consisting of a round liquid jet surrounded by a co-flowing annular gas stream. This fundamentally simple flow geometry provides for well-known exit conditions and avoids the complicated internal flows which are common to practical atomizers. A modular design was employed for the atomization test rig, which allowed for interchangeable gas nozzles and liquid tubes. Two different gas nozzles were chosen, consisting of a straight injector and a smooth-

convergence nozzle with a 12:1 contraction ratio. The latter nozzle provided for thin laminar boundary layers at the exit, which the straight geometry produced thicker turbulent boundary layers for the same flows. The liquid tubes used in the experiments had inner diameters of 1.0 mm and 0.32 mm, with the same outer diameter of 1.3 mm. The nozzle diameter for both gas nozzles was D_g = 11.2 mm, which yielded gas-to-liquid exit areas of approximately 125 and 1200 for the two liquid nozzles respectively.

The fluids chosen for this study were air for the gas flow, and both water and ethanol for the liquid. The section-averaged air velocity, U_g, was varied from 30 m/s to 165 m/s, while the liquid velocity was varied from 1.7 m/s to 16.6 m/s. All experiments were carried out at atmospheric pressure. Two measurement techniques were employed for the characterization of the liquid breakup process. Flow visualizations were performed using a high-speed digital video camera (Photron Super Fastcam) and stroboscopic backlight, while droplet size measurements were carried out at downstream locations ranging from x/D_g = 5 to 60 with a commercial phase-Doppler particle analyzer (PDPA) from TSI Incorporated.

3. Results

3.1 High-speed video observations

Select high-speed video images of the initial liquid jet breakup process at various flow conditions are shown in Fig. 2 a through 2c. The right side of each image corresponds to the nozzle exit plane, and the flow direction is therefore from left to right in all cases. The downstream extent of these images is approximately one gas-jet diameter. Fig. 2a is an image of the 1.0 mm water jet issuing at 1.7 m/s inside an annular gas flow with an exit velocity of 40 m/s. The liquid flow is laminar under these conditions, and the Weber number equals 24, which places the jet in a so-called 'membrane breakup' regime [1]. A well-defined wavelength of the primary shear instability (here of helical nature) is evident in this image. Fig. 2b presents the coaxial jet for the same liquid Reynolds number, but for a larger gas velocity of 69 m/s, which yields We = 74. The liquid jet is observed to make large radial excursions from the central axis, exposing segments of the jet to perpendicular exposure to the oncoming gas flow. In Fig. 2c, which corresponds to We = 437, the breakup process is much more intense, and the integrity of the liquid jet is compromised much closer to the nozzle exit. The liquid jet is effectively reduced to a fine mist over the lateral extent of the image. The breakup process in this image appears to be a strong stripping-type breakup which occurs on an intermediate scale associated with a secondary wave structure.

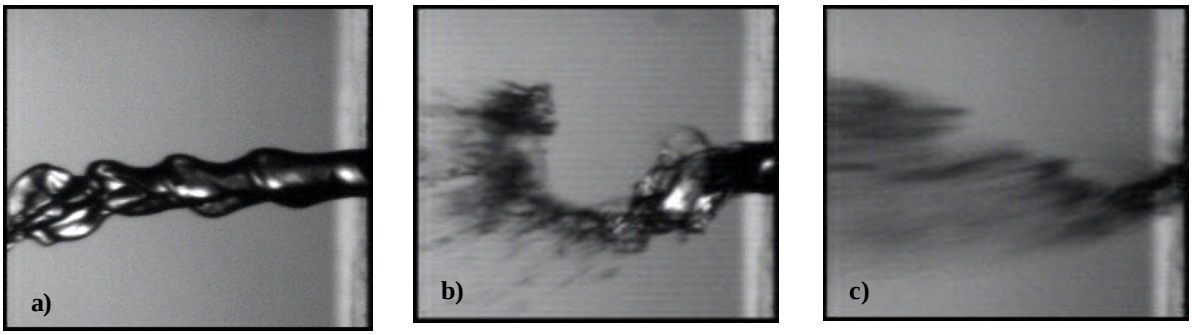

Figure 2 – Instantaneous initial breakup images, D_l = 1.0 mm a) U_g = 40 m/s, U_l = 1.7 m/s, We = 24, Re_g = 2.6 x 10^4, Re_l = 1700 b) U_g = 69 m/s, U_l = 1.7 m/s, We = 74, Re_g = 4.6 x 10^4, Re_l = 1700 c) U_g = 165 m/s, U_l = 1.7 m/s, We = 437, Re_g = 1.1 x 10^5, Re_l = 1700

3.2 Droplet-size measurements

In this subsection, results of droplet-size measurements taken at various locations downstream of the initial breakup region are presented. By varying flow conditions and fluid properties, an attempt has been made to determine the dependency of the *SMD* on various flow quantities. The sensitivity of the *SMD* to the liquid jet diameter for constant mass flux ratio is shown in Fig. 3, which is a plot of the droplet *SMD* as a function of x/D_g for water flow from two different nozzle diameters (D_l = 1.0 mm and 0.32 mm) and U_g = 165 m/s. This data indicates that the mean droplet size is not very sensitive to the liquid jet diameter, which was reduced by a factor of three between the two nozzles. Fig. 4 shows a comparison of the droplet *SMD* as a function of atomizing gas velocity at x/D_g = 15 for the two different gas nozzle geometries discussed in Section 2. A significant reduction in the *SMD* is observed for the convergent gas nozzle compared to the straight injector nozzle, with smaller diameters observed for the thin boundary layer associated with the convergent nozzle. The effect of surface tension on the *SMD* was investigated by comparing droplet-size measurements for the breakup of water and ethanol. Ethanol has a surface tension value which is approximately three times less than that of water, while possessing comparable density and viscosity values. Fig. 5 contains plots of droplet *SMD* as a function of x/D_g for water and ethanol jets emanating from the liquid tube of diameter D_l = 0.32 mm at U_l = 16 m/s. The gas exit velocity in these experiments was 165 m/s. Significantly smaller mean droplet sizes are observed for ethanol compared with water, and moreover, the size reduction appears to be a constant factor which is approximately $\sqrt{s_{water}/s_{ethanol}} \approx \sqrt{3}$. This result suggests a potential scaling of $SMD \mu We^{-1/2}$.

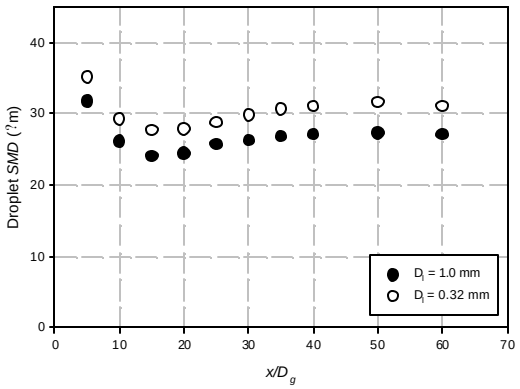

Figure 3 - Droplet *SMD* as a function of x/D_g for varying liquid jet diameter, U_g = 165 m/s

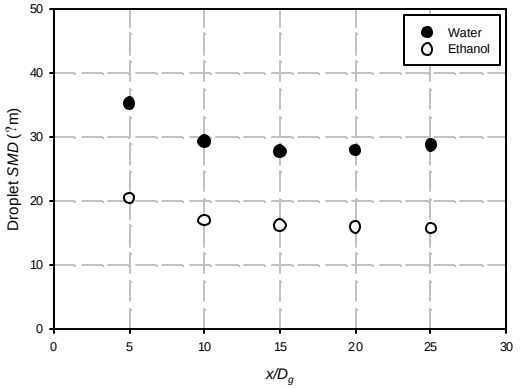

Figure 5 - Droplet *SMD* as a function of x/D_g for water and ethanol, D_l = 0.32 mm, U_l = 16

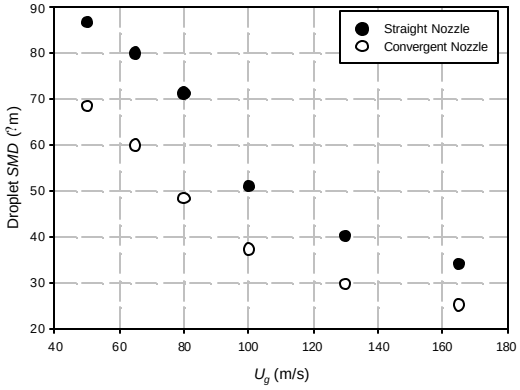

Figure 4 – Droplet *SMD* as a function of U_g for convergent and straight injector nozzles, D_l = 1.0 mm, U_l = 1.7 m/s, x/D_q = 15

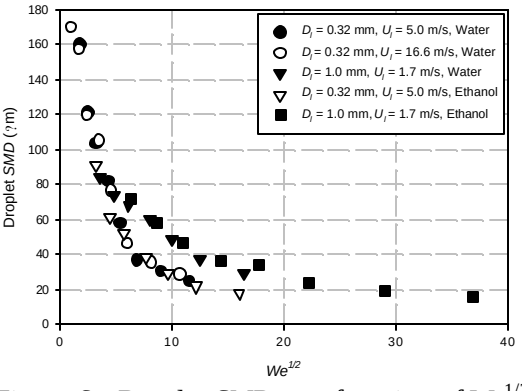

Figure 6 - Droplet *SMD* as a function of $We^{1/2}$

Fig. 6 contains five distinct droplet-size data sets which include measurements for water and ethanol, two different liquid nozzles, and various liquid nozzle exit velocities, all plotted as a function of $We^{1/2}$. The data collapse well to two distinct curves, one corresponding to each liquid jet diameter. As it will be shown in the following section, the critical length scale is the primary instability wavelength, l_1, rather than the liquid jet diameter. Recalling that this wavelength is proportional to the gas vorticity-layer thickness, we note that the measurements of Fig. 4. support this scaling, indicating an appreciable dependence of the *SMD* on the gas boundary-layer thickness.

4. Initial jet breakup model

Visual observations of the near-nozzle region of the coaxial liquid-gas jet flow in the present experiments have revealed a mechanism of jet breakup which appears to share common features with the disintegration of drops in high-speed gas streams. In particular, waves developed at the liquid jet surface by the primary shear instability in the coaxial jet are drawn out into tongues by the surrounding gas stream, and these tongues are subsequently destabilized in a manner which bears a striking resemblance to the accelerative destabilization of drops. This resemblance is illustrated in Fig. 7, which compares an image of coaxial jet breakup for the 1.0 mm diameter water jet (*We* = 437) in the current study to the breakup of a 2.5 mm water drop in a high-speed air stream [9]. The geometric resemblance of these two flow scenarios is shown schematically in Fig. 8. Primary wave surfaces exposed to the oncoming gas flow in the coaxial liquid-gas jet are roughly equivalent to one half of the windward surface of a liquid drop in a high-speed gas flow. Droplet formation appears to occur in both cases through the development of a secondary instability which manifests itself along the surface of the liquid tongues or the drop surface. The most plausible breakup mechanism, at least in the current experiments, appears to be associated with an accelerative destabilization of tongues of liquid drawn out of the jet surface by the primary shear instability; this accelerative destabilization mechanism being the well-known Rayleigh-Taylor instability which develops when a liquid surface is accelerated in a direction perpendicular to its plane. A phenomenological breakup model based on this instability mechanism is now presented.

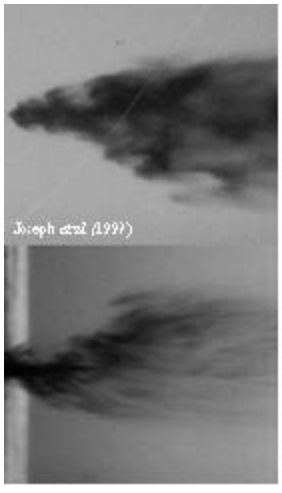

Figure 7 - Instantaneous flow image comparison of the catastrophic breakup of a 2.5 mm water droplet (Joseph *et al.* [9]) and a 1.0 mm water jet at high Weber number

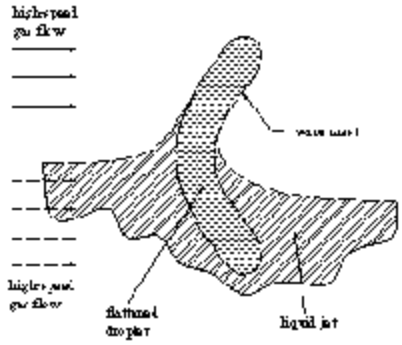

Figure 8 - Illustration of the analogy between high-speed gas flow over a liquid drop and over a primary wave crest in a coaxial liquid-gas jet

The action of the high-speed gas on the primary wave structure acts to draw the waves out into tongues of a characteristic thickness, proportional to l_1. The surfaces of these tongues are subsequently exposed to large accelerations by the high-speed gas stream, which destabilizes them via the Rayleigh-Taylor instability, forming corrugations of a characteristic wavelength, l_{RT}. These Rayleigh-Taylor waves become amplified, and the integrity of the liquid tongue is eventually broken, as droplets are formed with a typical size d, where $d \mu l_{RT}$. To develop this model, we consider the acceleration of the liquid tongue, perpendicular to its surface, at a constant acceleration, a. The classic linear stability analysis of the Rayleigh-Taylor problem, including the effects of surface tension [12], yields the following expression for the wave with the maximal growth rate:

$$l_{RT} = 2p\sqrt{3s/r_l a} \tag{4.1}$$

The acceleration of the liquid tongues, is estimated as

$$a \approx 10 r_g \left(U_g\left(1+\sqrt{r_g/r_l}\right)-U_l\right)^2 \Big/ r_l l_1 \tag{4.2}$$

Details of the development of this acceleration term can be found in [13]. The functional dependence of the primary wavelength on the density ratio and the vorticity-layer thickness was discussed in section 1, and can be written in general, as

$$l_1 = g\left(r_l/r_g\right)^{1/2}\left(n_g/U_g\right)^{1/2} \tag{4.3}$$

To estimate the proportionality constant, g, we have used experimental measurements of l_1 from images such as that shown in Fig. 2a. From this analysis, we have estimated g = 0.055m$^{1/2}$, which yields the following expression for the most unstable Rayleigh-Taylor wavelength,

$$l_{RT} \approx \frac{3.4 g^{1/2}\left(r_l n_g\right)^{1/4} s^{1/2}}{r_g^{3/4}\left[U_g\left(1+\sqrt{r_g/r_l}\right)-U_l\right]U_g^{1/4}} \tag{4.4}$$

In a manner similar to that which was done by Joseph et al. [9], predicted Rayleigh-Taylor wavelengths from Eq. 4.4 have been compared to measured values from a subset of our high-speed images. Two such images are presented here in Fig. 9 (additional comparisons may be found in [13]); in each figure, tick marks have been placed on the image to indicate the most evident wave spacing, which was measured using a commercial image analysis software program. In Fig. 9a, Eq. 4.4 predicts 242 µm, while the measured value was 200 µm. In Fig. 9b, the predicted wavelength is 185 µm, while the measured value was 213 µm. Over a larger subset of image comparisons, the agreement between Eq. 4.4 and the measured image values was on average within 14 percent.

A comparison of the *SMD* values to the measured Rayleigh-Taylor waves in our experiments suggests that (on average) $SMD \approx l_{RT}/5$, which permits the extension of Eq. 4.4 to provide a practical expression for the *SMD*,

$$SMD \approx \frac{0.68 g^{1/2}\left(r_l n_g\right)^{1/4} s^{1/2}}{r_g^{3/4}\left[U_g\left(1+\sqrt{r_g/r_l}\right)-U_l\right]U_g^{1/4}} \tag{4.5}$$

The dependence of the droplet *SMD* on surface tension predicted by the current model ($SMD \mu s^{1/2}$) is supported by the measurements presented in Section 3, and has been viewed here as a footprint of the Rayleigh-Taylor instability in the primary breakup process. The gas velocity dependence of this model is also significant, particularly in light of the historical

value which has been placed on correlations of the form, $SMD \mu U_g^{-n}$. Eq. 4.5 predicts a dependence of $U_g^{-5/4}$, or n = 1.25. Fig. 10 shows two plots of droplet *SMD* as a function of gas velocity in the current experiments, for two sets of flow conditions. Power-law curves have been fit to these data sets to determine the best-fit value of n for comparison to the model-predicted value of 1.25. The best fits to these data sets yield n =1.22 and 1.29, which agree very well with the model prediction.

A new Weber number may be defined based on the relevant length scale in the problem, l_1, as $We = r_g (U_g - U_l)^2 l_1 / s$, which for the case of interest, wherein $r_g << r_l$, permits Eq. 4.5 to be rewritten as

$$SMD / l_1 \approx 0.68 / We_{l_1}^{1/2} \qquad (4.6)$$

Fig. 11 contains the droplet-size data of Fig. 6, scaled by the primary instability wavelength, and re-plotted as a function of We_{l_1}. The data from the five different experiments, involving both water and ethanol, collapse very well over nearly a decade in We_{l_1} to the power law dependence predicted by Eq. 4.6.

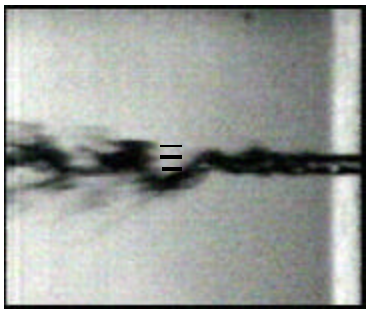

Figure 9 - Instantaneous flow image with identified Rayleigh-Taylor wavelengths, D_l = 0.32 mm, *We* = 37

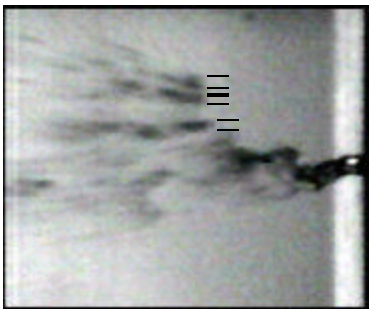

Figure 10 - Instantaneous flow image with identified Rayleigh-Taylor wavelengths, D_l = 0.32 mm, *We* = 47

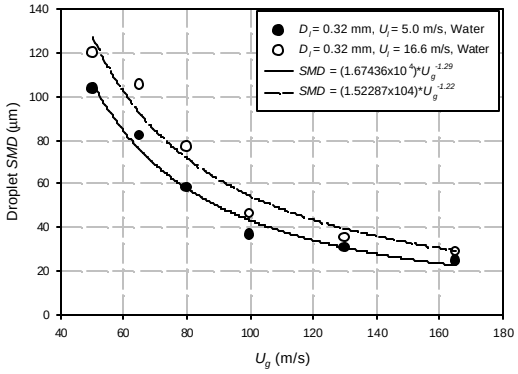

Figure 11 - Droplet *SMD* as a function of atomizing gas velocity

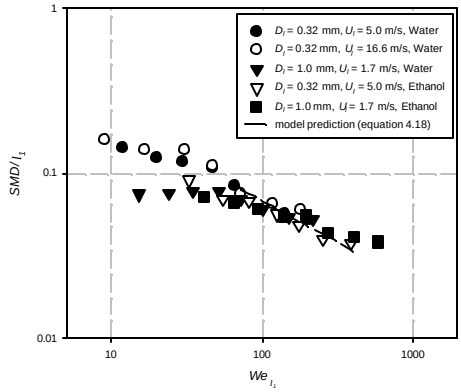

Figure 12 - Droplet SMD/l_1 as a function of We_{l_1}

5. Secondary mechanisms: Relative acceleration effects

Experimental data from coaxial liquid-gas jet flows consistently illustrates that the mean droplet diameter evolves with downstream distance from the nozzle outlet, indicating that additional processes are at work in the jet after the liquid droplets leave the near-nozzle primary breakup region. Fig. 13 contains *SMD* data as a function of x/D_g for the current coaxial configuration, and clearly exhibits this downstream variation of the mean drop size.

After the primary breakup process is completed, the *SMD* is observed to continue to decrease with downstream distance, eventually reaching a minimum value, and then subsequently increasing again gradually with continued downstream distance. A combined effect of several secondary mechanisms is typical in coaxial sprays, making it difficult to decipher which mechanism is dominant. These mechanisms can include such processes as turbulent breakup, droplet collisions, coalescence, evaporation, and relative acceleration. Along with the *SMD* evolution, Fig. 13 contains corresponding experimental measurements of the mean slip velocity between the largest droplets and the gas flow. The mean velocity of droplets of diameters $d < 5$ μm has been used to characterize the gas velocity. It is remarkable to note that the minimum *SMD* occurs at precisely the same downstream location as the maximum slip velocity of the largest size droplets. This observation supports the postulate that droplet acceleration plays more than a minor role in the downstream variation of the mean droplet diameter. A discussion of the quantitative effects of this mechanism can be found in [13] along with a comprehensive analysis of several other secondary breakup mechanisms.

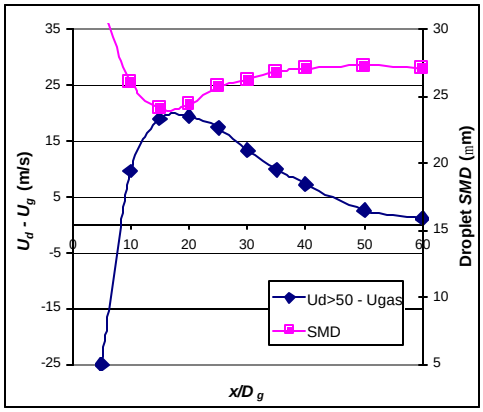

Figure 13 - Mean slip velocity for $d > 50$ μm and *SMD* as functions of x/D_g, $U_g = 165$ m/s, $U_l = 1.7$ m/s, $D_l = 1.0$ mm

6. *Conclusions*

The breakup and atomization of a small-diameter liquid jet by a high-speed gas stream has been shown to occur through a combined interfacial and Rayleigh-Taylor instability. A proposed Rayleigh-Taylor phenomenological breakup model based upon the acceleration of liquid tongues drawn out of the jet surface has been demonstrated to give results which agree very well with experimental mean droplet-size results for the breakup of both water and ethanol jets. Primary droplet sizes have been shown to scale well on the most unstable Rayleigh-Taylor wavelength, and the dependence of the droplet diameter on both the atomizing gas velocity and the liquid surface tension have been successfully captured by the proposed phenomenological breakup model.

7. *References*

[1] Lasheras, J.C. & Hopfinger, E.J. 2000 Liquid jet instability and atomization in a coaxial gas stream. *Annual Rev. Fluid Mech.* **32**, 275-308.

[2] Lefebvre, A.H. 1989 *Atomization and Sprays.* Hemisphere Publishing Corporation.

[3] Burick, R.J. 1972 Space storable propellant performance program. Coaxial injectors characterization. *NASA CR-120936*.

[4] Reitz, R.D. & Bracco, F.V. 1982 Mechanism of atomization of a liquid jet. *Phys. Fluids.* **25**(10), 1730-1742.

[5] Lin, S.P. & Lian, Z.W. 1989 Absolute instability of a liquid jet in a gas. *Phys. Fluids A.* **1**(3), 490-493.

[6] Mansour, A. & Chigier, N. 1991 Dynamic behavior of liquid sheets. *Phys. Fluids A.* **3**(12), 2971-2980.

[7] Lin, S.P. 1995 Regimes of jet breakup an breakup mechanisms (Mathematical aspects). In *Recent Advances in Spray Combustion: Spray Atomization and Drop Burning Phenomena*., ed. K. Kuo, **1**, 137-160.

[8] Raynal, L. 1997. *Instabilite et entrainement a l'interface d'une couche de mélange liquid-gaz.* These de Doctorat, Universite Joseph Fourier, Grenoble, France.

[9] Joseph, D.D., Belanger, J., & Beavers, G.S. 1999 Breakup of a liquid drop suddenly exposed to a high-speed air stream. *Int. J. Multiphase Flow* **25**, 1263-1303.

[10] Pilch, M. & Erdman, C.A. 1987 Use of break-up time data and velocity history data to predict the maximum size of stable fragments for acceleration-induced break-up of a liquid drop. *Int. J. Multiphase* Flow **13**, 741-757.

[11] Hsiang, L.P. & Faeth, G.M. 1992 Near-limit drop deformation and secondary breakup. *Int. J. Multiphase Flow* **18**, 635-652.

[12] Chandrasekhar, S. 1961. *Hydrodynamic and Hydromagnetic Stability*. Clarendon Press, Oxford.

[13] Varga, C.M. 2002. *Atomization of a small-diameter liquid jet by a high-speed gas stream.* Doctoral Thesis, University of California, San Diego, La Jolla, California.